AIAA JOURNAL
Vol. 38, No. 3, March 2000

Smoothed Sensitivity Equation Method for Fluid Dynamic Design Problems

Andrea Dadone*
Politecnico di Bari, 70125 Bari, Italy
Mauro Valorani†
University of Rome "La Sapienza," 00184 Rome, Italy
and
Bernard Grossman‡
Virginia Polytechnic Institute and State University, Blacksburg, Virginia 24061

We consider shape optimization problems involving compressible fluid flows, which are characterized by nonsmooth and/or noisy objective functions. Such functions are difficult to optimize using derivative-based techniques. To overcome such a difficulty, we suggest an approach for estimating the sensitivity derivatives, based on a suitable smoothing of the sensitivity equations. The smoothing affects only the sensitivity derivatives and not the accuracy of the analysis. The basic mechanism by which the smoothing process achieves this result is illustrated with the help of an inverse design problem involving an inviscid quasi-one-dimensional flow having a closed-form solution. The convergence properties and the computational efficiency of the approach are demonstrated on two inverse design problems involving two-dimensional inviscid, compressible flows.

Introduction

FLUID dynamic design problems require the calculation of many computationally expensive flow analyses. It is vital to make the optimization strategy as efficient as possible. This requirement is even more important for situations when the objective functions are noisy or nonsmooth, which may compromise or even prevent the convergence of standard optimization techniques. Noise can be caused both by changes in the computational mesh (for example in problems with free boundaries) and by poor convergence properties of the numerical scheme (as may occur when using flux limiters in upwind shock-capturing schemes). Nonsmoothness may be created by the presence of flow discontinuities, such as shock waves, contact discontinuities, and slip lines because these are represented on a discrete computational mesh. When these discontinuities are accurately represented, a change in some design parameters may force them to move from one cell to another, and this change may cause large variations in the objective function. All of the outlined situations may result in objective functions with several local minima.

Gradient-based optimization techniques require the gradient or, using a different terminology, the sensitivity derivatives of the objective function with respect to the design variables. A general description of these methods may be found, for example, in Ref. 1. The most common technique to estimate the sensitivities is based on finite differences of the results of several flow analyses. The main drawbacks of this approach are the large number of flow analyses involved and questions of accuracy.

Beside the standard finite difference (FD) method (the black-box approach), there exist more efficient ways of computing the sensitivity derivatives of the objective function.

These alternate methods are the sensitivity equations method (SEM), also referred to as the direct formulation of the sensitivity equations, and the adjoint methods (AM).

The direct formulation of the sensitivity equations[2] involves differencing the state equations and using the chain rule to find sensitivity derivatives of the objective function. This method requires only one flow solution and the solving of N_v sets of linear (direct) sensitivity equations, where N_v is the number of design variables used to parameterize the design problem.

The adjoint formulation of the sensitivity equations[3,4] resorts to a formulation inherited from the control theory. It requires only one flow solution and the solution of only one set of linear adjoint equations.

These methods are more efficient than the standard FD method mainly because only one flow solution is required to compute the sensitivity derivatives instead of the $N_v + 1$ (or $2N_v + 1$ for second-order accuracy) flow solutions needed by the FD method. The sensitivity or adjoint equations can be derived from the flow equations written in either the continuous or discrete forms, as presented in Refs. 5 and 6.

However, the nonsmoothness of the objective function may present difficulties for the convergence of these gradient-based optimization process.

The one-dimensional flow in a transonic diffuser has been considered in Ref. 7. The objective function was computed by using different flow solvers. A staircase plot was obtained by using an exact flow solver, with large regions of positive slopes at the left of the design value. The connection between the staircase pattern and the shock has also been demonstrated. Two procedures for treating the nonsmoothness were presented, one involving shock fitting and the other coordinate straining. Reference 7 also showed that the objective function plot tends to become smooth if a centered scheme is employed with a sufficiently high level of artificial viscosity, which smears the shock over many mesh cells. At the same time the accuracy of the solution may be severely degraded.

A response surface methodology[8] circumvents this problem by interpolating the objective function by means of quadratic polynomials. The response surface was periodically updated in order to approach an accurate optimal solution of the original inverse problem. A drawback of this procedure is that the number of analyses grows rapidly as the number of design variables increases.

The adjoint procedure used by Jameson[4] uses a centered scheme that has smoother convergence properties than flux-limited upwind schemes. Shocks are typically smeared over four mesh cells, and the procedure followed in Ref. 4 involves the smoothing or filtering of the objective function, which could affect the location of the computed optima.

Received 8 January 1999; revision received 25 June 1999; accepted for publication 5 July 1999. Copyright © 1999 by the authors. Published by the American Institute of Aeronautics and Astronautics, Inc., with permission.

*Professor and Department Head, Istituto di Macchine ed Energetica. Senior Member AIAA.

†Associate Professor, Dipartimento di Meccanica ed Aeronautica. Member AIAA.

‡Professor and Department Head, Department of Aerospace and Ocean Engineering. Associate Fellow AIAA.

In this work we present an approach to estimate the sensitivity derivatives of the nonsmooth objective function. This goal is achieved by introducing a set of smoothed sensitivity equations (SSE) obtained by modifying the set of the original sensitivity equations by adding an artificial dissipative term.[8–10] The optimization search is performed on the basis of the original nonsmooth objective function and of the smoothed sensitivity derivatives (SSD) obtained by solving the set of SSE.

The suggested approach is shown to be effective and efficient in the design of a transonic diffuser by using quasi-one-dimensional inviscid flow equations. This test problem was first introduced by Frank and Shubin[5] and studied by others, i.e., Refs. 6, 7, and 11–13. The one-dimensional problem will serve to illustrate how the proposed approach becomes successful in handling the class of flow design problems involving nonsmooth objective functions.

Then the approach will be validated in two-dimensional flows. Two design problems involving Euler flow solutions will be considered: 1) the extension to two dimensions of the diffuser design problem discussed in the context of the one-dimensional flow model and 2) a problem involving the inverse design of a nozzle, originally considered in Ref. 14.

Defining the Cost Function

All inverse design problems considered in this paper involve finding a vector of N_v design variables $\boldsymbol{\xi}$, which allows the reconstruction of the shape A of a duct, either a diffuser or a nozzle, such that some known function F of the flow solution $\boldsymbol{q}(\boldsymbol{x}, \boldsymbol{\xi})$, which depends on the position vector $\boldsymbol{x}$ and the design variables $\boldsymbol{\xi}$, will approach as closely as possible a prescribed target distribution $\hat{F}$. The function F can be defined as the Mach number M, the flow velocity u, or the pressure p. In turn, the flow solution $\boldsymbol{q}$ is defined as a vector-valued function, which is the solution of a set of partial differential equations describing an inviscid compressible flow. An optimization search starting from a first guess $\boldsymbol{\xi}_0$ will find the vector $\hat{\boldsymbol{\xi}}$ yielding the minimal error between F and $\hat{F}$ over a given domain D. The search can be driven by an objective, or cost, function I defined as the error between the two F distributions:

$$I[\boldsymbol{q}(\boldsymbol{x}, \boldsymbol{\xi}), \boldsymbol{\xi}] = \frac{1}{2S} \int_D \{F[\boldsymbol{q}(\boldsymbol{x}, \boldsymbol{\xi})] - \hat{F}[\hat{\boldsymbol{q}}(\boldsymbol{x})]\}^2 \, \mathrm{d}\boldsymbol{x} \tag{1}$$

where S is the area of D, $\boldsymbol{x}$ is a position vector in the N_{ps}-dimensional physical space, and $\boldsymbol{\xi}$ is the vector of design variables having N_v dimensions.

The target F distribution for all tests considered in this paper can be exactly recovered by the specific choice of design variables adopted. Thus, the optimal distance I for all cases is always zero, and a vector $\hat{\boldsymbol{\xi}}$ always exists that makes $\boldsymbol{q}(\boldsymbol{x}, \hat{\boldsymbol{\xi}})$ correspond exactly to $\hat{\boldsymbol{q}}(\boldsymbol{x})$. This allows the association of a target area distribution $\hat{A} = A(\boldsymbol{x}, \hat{\boldsymbol{\xi}})$ to the target distribution $\hat{F}$.

Smoothed Sensitivity Equations

The analysis of the design problems involving flows with shocks is simpler if it is carried out with reference to a quasi-one-dimensional flow model. The findings obtained in this framework can be easily extended to two-dimensional flows as described later in this paper. This section will illustrate the rationale for introducing the smoothed sensitivity derivatives.

Inverse Design of a Transonic Diffuser

The analysis will be carried out with reference to a test case involving the inverse design of a transonic diffuser of unit length (Fig. 1) having a prescribed target area distribution $\hat{A}$. For this test case the function F in Eq. (1) is the flow velocity u. The domain D along which the target distribution is prescribed is the interval $(O - L)$ along the x axis, whose size is independent of the design variables.

The duct shape is parameterized by a set of N_v design variables $\boldsymbol{\xi}$, which are defined as the cross-section areas of the duct at a selected location along the x axis. The area distribution $A(x)$ is defined by cubic spline interpolation of the design variables as shown in Fig. 1. Up to seven design variables are considered for this test ($1 \leq N_v \leq 7$).

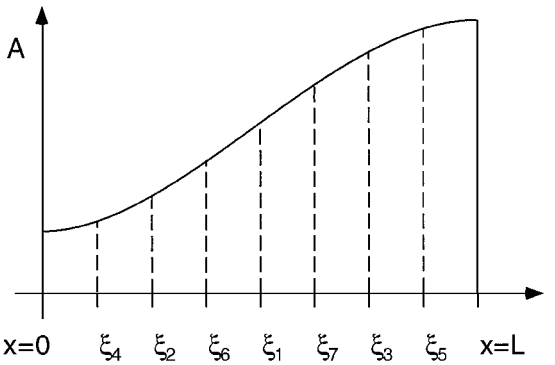

Fig. 1 Transonic diffuser test case.

The target area distribution for the one-dimensional case is defined by $\hat{A}(x) = -1.390x^3 + 2.085x^2 + 1.050$. The velocity at the inlet and exit boundaries is 1.299 and 0.506, respectively, as in Refs. 4–8. Zero slope of $A(x)$ is enforced at both duct ends to determine the spline uniquely.

Closed-Form Solution of the Flow Model

If the flow in the diffuser is assumed inviscid, steady, and quasi-one dimensional and the fluid a perfect gas, then the Euler equations can be reduced to a single ordinary differential equation in the unknown flow velocity $u(x)$ (Ref. 5):

$$w(u, x; \xi) = \frac{\mathrm{d}f(u)}{\mathrm{d}x} + g[u, A(x; \xi)] = 0 \tag{2}$$

where x varies from 0 to L, the duct length; γ is the ratio of specific heats set equal to 1.4; A is the cross-section area of the duct; and the functions f and g are defined as

$$f(u) = u + \frac{(\gamma - 1)}{(\gamma + 1)} \frac{2h_0}{u}$$

$$g(u, A) = \frac{A_x}{A} \frac{(\gamma - 1)}{(\gamma + 1)} \left(u - \frac{2h_0}{u} \right) \tag{3}$$

The total enthalpy per unit mass h_0 is normalized by the square of the speed of sound at the inlet, A by the square of L, x by L, and u by the inlet speed of sound. The solution u depends on x and $\boldsymbol{\xi}$ through the area because $A(x{:}\boldsymbol{\xi})$.

Equation (2), under these assumptions, has a closed-form solution reported in Refs. 5 and 6. In transonic flows the shock position is found by enforcing the Rankine–Hugoniot relation across the normal shock.

The closed-form solution is used for the one-dimensional flow model. The two-dimensional flow model formulation uses numerical solutions of the flow equations.

Sensitivity Equation

If the direct continuous form of the sensitivity equation is adopted and if only one design variable is considered, then one can obtain the sensitivity derivative $\mathrm{d}I/\mathrm{d}\xi$ of the objective function $I[u(x, \xi), \xi]$—defined in Eq. (1)—with respect to the design variable ξ by writing

$$\frac{\mathrm{d}I}{\mathrm{d}\xi} = \frac{1}{S} \int_D [u(x, \xi) - \hat{u}(x)] \frac{\mathrm{d}F}{\mathrm{d}u} \frac{\mathrm{d}u}{\mathrm{d}\xi} \, \mathrm{d}x + \frac{\partial I}{\partial \xi} \tag{4}$$

In Eq. (4), $\mathrm{d}F/\mathrm{d}u = 1$ and $\partial I/\partial \xi = 0$ because $F = u$ and I does not depend on ξ explicitly. The unknown in Eq. (4) is the flow sensitivity $u' \equiv \mathrm{d}u/\mathrm{d}\xi$. To find u', Eq. (2) is differentiated with respect to ξ to yield

$$\frac{\mathrm{d}w}{\mathrm{d}\xi} = \frac{\mathrm{d}}{\mathrm{d}\xi} \left(\frac{\mathrm{d}f}{\mathrm{d}x} \right) - \frac{\mathrm{d}g}{\mathrm{d}\xi} = 0 \tag{5}$$

Formally the derivation with respect to ξ and x in Eq. (5) can be inverted to yield

$$\frac{\mathrm{d}}{\mathrm{d}x} \left(\frac{\mathrm{d}f}{\mathrm{d}u} \frac{\mathrm{d}u}{\mathrm{d}\xi} \right) + \frac{\mathrm{d}g}{\mathrm{d}u} \frac{\mathrm{d}u}{\mathrm{d}\xi} - \frac{\partial g}{\partial \xi} = 0 \tag{6}$$

where df/du and dg/du are evaluated at $\bar{u}$, which is the closed-form solution to Eq. (2). By denoting $a \equiv df/du$, $b \equiv dg/du$, and finally $g' \equiv dg/d\xi$, we obtain

$$\frac{d}{dx}\{a[\bar{u}(x)]u'(x)\} = -b[\bar{u}(x), A(x)]u'(x) - g'[\bar{u}(x), A(x)] \quad (7)$$

Equation (7) yields continuous solutions $u'(x)$ only if the flow solution $\bar{u}(x)$ is smooth; otherwise both the coefficients $a(x)$ and $b(x)$ become nondifferentiable across the shock. When this happens, a solution of Eq. (7) can be found only by resorting to a weak formulation of it.

In fact, one can easily make a heuristic argument that the flow sensitivity $u' = du/d\xi$ develops a δ function as a consequence of the presence of a shock in the flow solution $\bar{u}$.

By applying a small perturbation $\delta\xi \approx \mathcal{O}(\epsilon)$ to the design variable ξ, the shock moves along the nozzle by a small distance $\delta x \approx \mathcal{O}(\epsilon)$. However, the change of velocity across the shock δu is finite, that is, of order one. Now, consider a point of the duct where the flow regime, because of the shock displacement, switches from subsonic to supersonic, or vice versa. There, the order of magnitude of the flow sensitivity becomes $\delta u/\delta\xi \approx \mathcal{O}(1)/\mathcal{O}(\epsilon)$, which tends to infinity as $\delta\xi$ tends to zero.

The contribution of this δ function to the sensitivity derivative $dI/d\xi$, defined as an integral over the domain D [Eq. (4)], dominates over that of the smooth part of the flow. Therefore, the sensitivity derivative takes the correct sign to drive the optimization process to convergence only if the δ function is properly accounted for.

Weak Formulation of the Sensitivity Equation

The weak form of Eq. (7) can be obtained by choosing any continuously differentiable test function $\Phi(x)$ with compact support on a domain Ω, which includes D. Thus, on a domain Ω the following relation holds:

$$\int_\Omega \frac{d}{dx}[a(x)u'(x)]\Phi(x)\,dx = -\int_\Omega [b(x)u'(x) - g'(x)]\Phi(x)\,dx \quad (8)$$

Integrating by parts, the integral on the left-hand side yields

$$a(x)u'(x)\Phi|_{\partial\Omega} - \int_D [a(x)u'(x)]\frac{d\Phi(x)}{dx}\,dx = -\int_D [b(x)u'(x) - g'(x)]\Phi(x)\,dx \quad (9)$$

However, the first term vanishes because Φ has compact support over Ω and the integral term requires that u' be a measurable function. A function $\bar{u}'(x)$, which satisfies Eq. (9), is a weak solution of Eq. (7).

Entropy Solutions of the Sensitivity Equation

The weak solution of Eq. (9) is not unique, and a physically meaningful solution can be selected by prescribing that the weak solution has to satisfy an entropy condition.

One way to find the entropy-satisfying solution is to modify Eq. (7) by adding to it an artificial viscosity term as follows:

$$\frac{d}{dx}[a(x)u'(x)] + b(x)u'(x) + g'(x) = \alpha\frac{d^2u'(x)}{dx^2} \quad (10)$$

A solution $u'(x)$ of Eq. (10) exists and is unique and smooth: it will be denoted as $u'_\alpha(x)$. As α tends to zero, $u'_\alpha(x)$ tends to $\bar{u}'(x)$, which is an entropy-satisfying weak solution of Eq. (7). If α is a constant, then Eq. (10) can be rewritten as a smoothed sensitivity equation:

$$\frac{d}{dx}\left(a(x)u'(x) - \alpha\frac{du'(x)}{dx}\right) + b(x)u'(x) + g'(x) = 0 \quad (11)$$

Auxiliary Flow Equation

Instead of altering the sensitivity equation, Eq. (7), it is possible to modify the original flow equation, Eq. (2), so as to recover the same result expressed by Eq. (11). This turns out to be a simpler way to implement the concept of smoother sensitivity equations.

If an artificial viscosity term ν having the form

$$\nu(u;\alpha) = \alpha\frac{d^2u}{dx^2} \quad (12)$$

where $\nu(u;\alpha)$ depends only on u and not explicitly on ξ, is added to the original flow equation (2), one obtains the modified equation:

$$W(u, x; \xi; \alpha) = w(u, x; \xi) - \nu(u;\alpha) = 0 \quad (13)$$

This expression can be differentiated with respect to the design variable ξ. However, the order of derivation in $dw/d\xi$ and $d\nu/d\xi$ can be reversed according to the identity

$$\frac{d}{d\xi}\left(\alpha\frac{d^2u}{dx^2}\right) = \alpha\frac{d^2}{dx^2}\left(\frac{du}{d\xi}\right) \quad (14)$$

for u'_α being a smooth function. If α is a constant with respect to x, then the sensitivity equation of Eq. (13) coincides with Eq. (11).

This can be better appreciated once the identity

$$W = w - \nu = \frac{d\tilde{f}}{dx} - g = 0 \quad (15)$$

is established by introducing the modified flux $\tilde{f}$, defined as

$$\tilde{f} = f - \alpha\frac{du}{dx} \quad (16)$$

To summarize, a procedure to find a physically meaningful (entropy-satisfying) weak solution of Eq. (9) requires the addition of an artificial viscosity term to Eq. (7) so as to obtain Eq. (11); however, Eq. (11) coincides with the sensitivity equation of Eq. (2) after the flux f is substituted by $\tilde{f}$ according to Eq. (16).

The modified flux $\tilde{f}$ is the same introduced to solve flows with shocks by means of centered schemes. However, in this paper the artificial viscosity is used only to obtain the approximate flow sensitivity $u'_\alpha(x)$ that could effectively lead to the optimum of the nonsmooth objective function even when flow discontinuities make the data $a(x)$ and $b(x)$ discontinuous. Therefore, there is no attempt to regularize the objective function by smoothing the discontinuous flow solution or to filter the objective function as done in Refs. 4, 11, and 12.

The concept of modifying the sensitivity equations while the original objective function is kept unchanged can be equally applied to both the analytic and the discrete formulations written according to both the direct and the adjoint methods.

Discrete Analysis

This section will illustrate how the idea of the smoothed sensitivity equations introduced by resorting to the continuous direct formulation of the sensitivity equations can be implemented in the discrete direct and adjoint formulations.

Discrete Cost Function

First, Eq. (1) has to be discretized. If the trapezoid rule is adopted, one obtains

$$I[\boldsymbol{q}_i(\boldsymbol{\xi}), \boldsymbol{\xi}] = \frac{1}{2\tilde{S}}\sum_{i=1}^{N_d}\{F[\boldsymbol{q}_i(\boldsymbol{\xi})] - \hat{F}[\hat{\boldsymbol{q}}_i]\}^2\Delta\boldsymbol{x}_i \quad (17)$$

where N_d is the total number of cells of the mesh that discretizes D, $\boldsymbol{x}_i$ is the position vector of the cell centroid, $\Delta\boldsymbol{x}_i$ is the area of the ith cell, $\boldsymbol{q}_i(\boldsymbol{\xi}) = \boldsymbol{q}(\boldsymbol{x}_i, \boldsymbol{\xi})$ and $\hat{\boldsymbol{q}}_i = \hat{\boldsymbol{q}}_i(\boldsymbol{x}_i)$, and finally

$$\tilde{S} = \sum_{i=1}^{N_d}\Delta\boldsymbol{x}_i$$

approximates the area of D.

Discrete SSE

The discrete direct (DD) and adjoint (DA) formulations obtained by starting from the discrete objective function (17) and the discrete flow equation can be found in Ref. 9, whereas the modified flow equation (15) can be formally approximated at the kth mesh point by the expression

$$W_k(u_i, \xi; \alpha) = w_k(u_i; \xi) - v_k(u_i; \alpha)$$

$$= \frac{\delta \tilde{f}_k(u_i; \alpha; \xi)}{\delta x} + g_k(u_i; \xi) = 0 \tag{18}$$

with k ranging from 1 to N_d. The finite difference approximation in Eq. (18) can be written according to a cell-centered finite volume formulation to yield

$$W_k(u_i, \xi; \alpha) = \frac{\tilde{f}_{k+\frac{1}{2}} - \tilde{f}_{k-\frac{1}{2}}}{\Delta x} + g_k = 0 \tag{19}$$

The fluxes $\tilde{f}$ may be discretized as

$$\tilde{f}_{k+\frac{1}{2}} = \tfrac{1}{2}[f_{k+1} + f_k - \alpha(u_{k+1} - u_k)] \tag{20}$$

where $f_{k+1} = f(u_{k+1})$, etc., and α is a parameter controlling the amount of artificial dissipation. The flow velocity u_i at the location x_i is obtained from the closed-form solution of Eq. (2).

Following the discrete direct formulation, Eq. (19) is differentiated with respect to the design parameter ξ to yield N_v linear systems of the form

$$\frac{\partial W_k}{\partial u_i}\frac{\partial u_i}{\partial \xi_j} = -\frac{\partial w_k}{\partial \xi_j} \tag{21}$$

with j from 1 to N_v, whereas if we follow the discrete adjoint formulation a single system is obtained:

$$\left(\frac{\partial W_k}{\partial u_i}\right)^T \lambda^k = -\frac{\partial I}{\partial u_i} \tag{22}$$

where λ^k are the Lagrange multipliers.

The artificial dissipation affects only the matrices of the linear systems (21) and (22) because $\partial W_k/\partial \xi_j$ coincides with $\partial w_k/\partial \xi_j$ being v independent of ξ_j. Thus, the addition of dissipation can be viewed as a means to modify the Jacobian of the systems (21) and (22), which become ill-conditioned when the flow solution develops shocks.

The δ function can be detected in the discrete formulation by approximating the flow sensitivity u' by finite differences. All calculations reported in Fig. 2a refer to the quasi-one-dimensional flow model; only one design variable, ξ, defined as the cross-section area at midlength of the duct, is considered. The flow velocity distribution involving a shock is found by the closed-form solution of Eq. (2) and injected onto a computational mesh having 64 cells. Thus, the data $a(x)$ and $b(x)$ of Eq. (7) are discontinuous across the shock.

Figure 2a shows that a large peak is located where the flow develops a shock wave. This peak is the numerical approximation of the δ function whose height increases as $\Delta\xi$ is reduced.

However, the FD-based flow sensitivity can capture the δ function only if $\Delta\xi$ can force the shock to move beyond at least one cell of size Δx. Indeed, the FD flow sensitivity will capture the peak only when two flow solutions presenting a shock at two different cells are compared. This is confirmed by setting $\Delta\xi = 0.001$ (Fig. 2a) With such a small $\Delta\xi$, the shock stays in the same cell despite the perturbation, and the FD flow sensitivity will present only a jump in front and behind the original and the perturbed shock location but not the peak. Without this peak the contribution to the overall sensitivity is underestimated and the sign of $\mathrm{d}I/\mathrm{d}\xi$ becomes incorrect.

The SSE method may overcome the limits of finite differences and lead to meaningful approximation of the sensitivity derivatives. Figure 2b shows that the SSE formulation with the cell-centered scheme (20) can actually capture the peak, whereas the FD method cannot. Increasing the amount of dissipation α broadens and lowers the peak. Consider, however, that the FD flow sensitivity, elsewhere than at the missed peak, is accurate. Thus, Fig. 2b shows that the SSE-based flow sensitivities away from the shock become less accurate as α is increased. The effect of the peak spreads over a large portion of the domain when the SSE approach is used. This effect may be thought of being caused by the second-order operator adding an elliptic character to the originally hyperbolic partial differential equations (PDEs). However, attempts to improve the performance of the SSE method by adopting upwind-biased instead of cell-centered schemes showed that only the latter type of scheme (or some variation of it) can capture numerically the δ function.

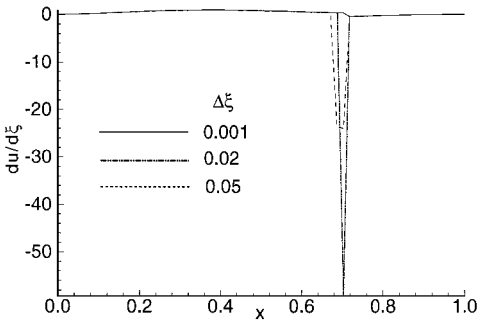

a) Numerical flow sensitivity du/dξ obtained by using different increments of the design parameter $\Delta\xi$

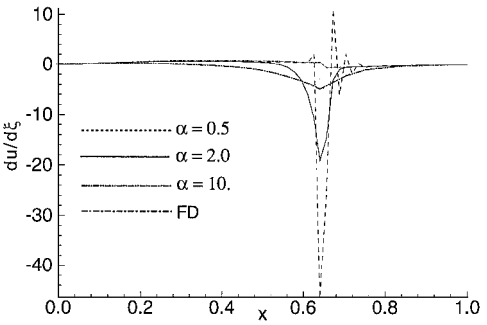

b) du/dξ obtained by the FD and SSE methods

Fig. 2 Discrete SSE.

Quasi-One-Dimensional Diffuser

This section presents results for the inverse design of a transonic diffuser when a quasi-one-dimensional flow model is used to find the flow solution. First, the nonsmooth nature of the objective function is demonstrated. Next, the results relative to the application of the SSE method are reported.

Objective Function

The aim of this section is to show that the objective function driving the inverse design problem of a transonic diffuser is nonsmooth. If the shape of the duct is parameterized with a single design variable placed at one-half of the duct length, we can easily visualize the objective function $I(\xi)$ (Fig. 3). The closed-form flow solution is used to compute the flow velocity through the duct. In Fig. 3 we can observe the staircase pattern of the objective function obtained by meshes with different number of cells. The jumps in the objective function result from the interaction of the shock wave and the numerical evaluation of the integral in the objective function. Note that increasing the resolution does not alleviate the problem. In contrast, higher resolutions yield many more jumps and local minima, although of reduced height. A more in-depth explanation of this phenomenon is found in Ref. 7.

FD vs SSE Sensitivity Derivatives

The validity of the SSE approach will be demonstrated by comparing the FD sensitivity derivatives with those obtained by the SSE method. In this example, the target value $\hat{\xi}$ is set at 1.3975. Figure 4a shows the comparison of the sensitivity derivative $\mathrm{d}I/\mathrm{d}\xi$ computed by FD and by the SSE method with a different amount of dissipation.

The results show that, where the finite differences can be defined, that is, everywhere but at the jumps, they have positive values both before and after the target value $\hat{\xi}$. Clearly, optimization starting from the left of the target will not converge to the optimum design.

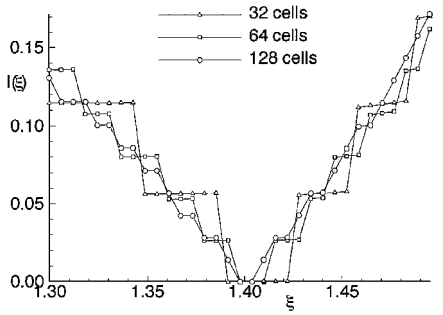

Fig. 3 Nonsmooth objective functions as a function of mesh cell size.

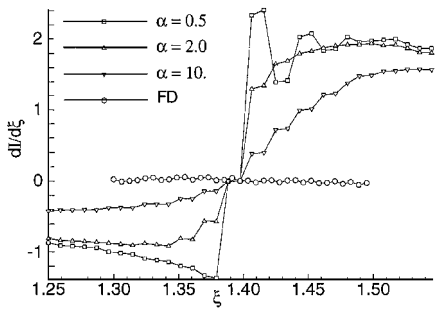

a) FD vs SSE sensitivity derivatives

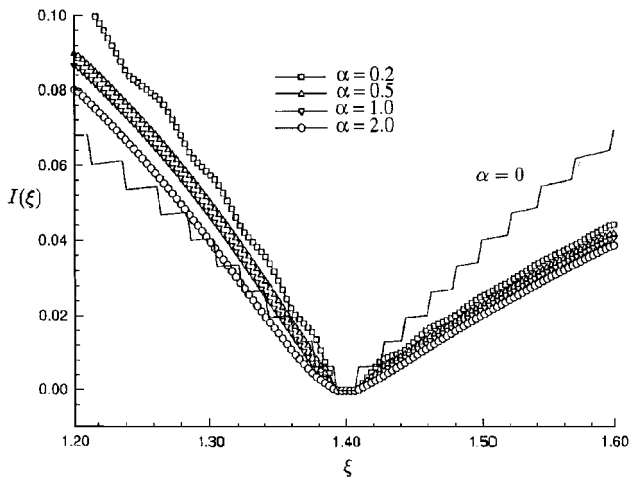

b) Original objective function compared to the numerical integrals of the sensitivity derivatives obtained by the SSE method

Fig. 4 FD and SSE sensitivity derivatives.

In contrast, the SSE method provides negative slopes at the left of the target value and positive at its right. Moreover, the slope of the sensitivity derivatives, although being still nonsmooth, is defined at every value of ξ. For this case a derivative-based optimization will converge only if the sensitivity derivatives are computed by the SSE method.

The numerical integrals of the SSE sensitivity derivatives, despite their being obtained by using a centered scheme, turn out to be very similar to the objective functions obtained by using a relatively nondissipative solver, such as the Godunov scheme.[7] The numerical integrals are compared to the original objective function in Fig. 4b. The SSE approach produces sensitivity derivatives that can be thought of as being the derivatives of a filtered objective function, with the advantage of not needing to actually carry out the filtering.

SSE Convergence Properties

To test the sensitivity derivatives obtained by the SSE method, we report two optimizations related to the same test case but for a different number of design variables: $N_v = 1$ and 7. The optimization uses a Newton method for the one-design-variable case and a combination of Newton-like methods for the seven-design-variable case.

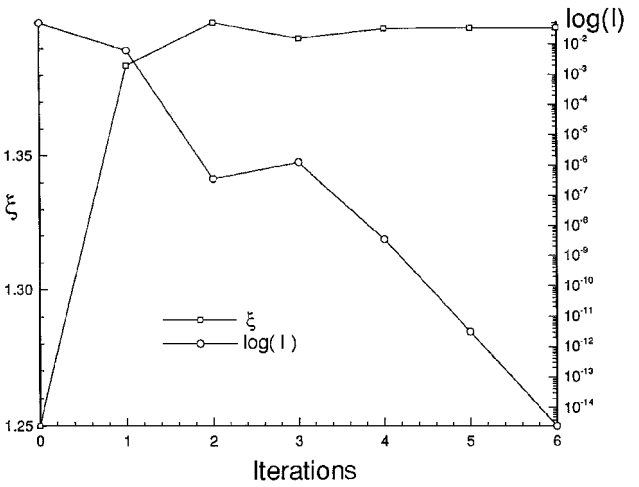

a) One design parameter

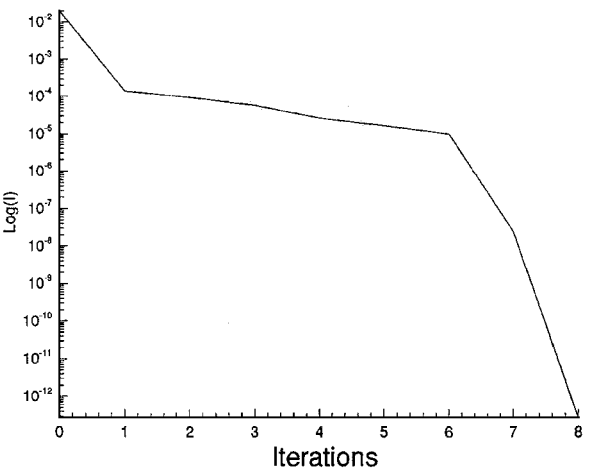

b) Seven design parameters

Fig. 5 Convergence histories for the quasi-one-dimensional transonic diffuser.

First, we consider a design problem with a single design variable placed at the middle of the duct. The target value of the design variable is $\hat{\xi} = 1.3975$. The starting point is arbitrarily chosen at $\xi_0 = 1.25$. Then, we consider a test with seven design variables, located evenly throughout the length of the duct. The target area distribution is the same as in the one-design-variable case.

Convergence histories of the optimization for the one- and seven-design-variable cases are shown in Figs. 5a and 5b, respectively. The figures report the history of the objective function and for the one-design-variable case only the design variable as it varies during the iterations of the optimization process (Fig. 5a). For the one- and seven-design-variable cases the SSE method is able to reduce the objective function to double precision machine zero, that is, to recover the target velocity distribution exactly in fewer than 10 iterations.

Extension to Two-Dimensional Problems

The extension of the SSE method to two-dimensional problems is straightforward. The flow solution is obtained by adopting the finite volume flux-difference splitting method,[15] with an approximate Riemann solver to capture the shock waves accurately. A MUSCL-type upwind extrapolation method, formally second-order accurate in space, extrapolates the physical variables onto the left and right sides of each cell edge. The Van Albada limiter ensures oscillation-free solutions. The computational flowfield is discretized into a $N_m = N_x \times N_y$ finite volume mesh, where N_x denotes the cells used in the streamwise direction and N_y the cells in the crossflow direction.

A different solver is chosen to compute the sensitivity derivatives. The simplest scheme that will meet our goal is a cell-centered finite volume scheme with an adequate level of artificial viscosity. Within the context of a two-dimensional Cartesian formulation, we can modify the flux at a generic $(i + \frac{1}{2}, j)$ cell edge with the introduction of artificial viscosity. This modifies the corresponding $\boldsymbol{F}_{i+1/2,j}$ flux by subtracting an artificial viscosity flux $\boldsymbol{D}_{i+1/2,j}$. At this cell edge the total flux $\tilde{\boldsymbol{F}}_{i+1/2,j}$, per unit length, is given by

$$\tilde{\boldsymbol{F}}_{i+\frac{1}{2},j} = \boldsymbol{F}_{i+\frac{1}{2},j} - \boldsymbol{D}_{i+\frac{1}{2},j} \tag{23}$$

where a very simple form of artificial viscosity suffices to obtain useful sensitivity derivatives, that is,

$$\boldsymbol{D}_{i+\frac{1}{2},j} = \alpha \tilde{I}(\hat{\boldsymbol{q}}_{i+1,j} - \hat{\boldsymbol{q}}_{i,j}) \tag{24}$$

where $\tilde{I}$ is the identity matrix. The vector $\hat{\boldsymbol{q}}$ collects the conserved variables, defined as

$$\hat{\boldsymbol{q}} = [\rho, \rho u, \rho v, \rho e^0]^T \tag{25}$$

The flux $\boldsymbol{F}_{i+1/2,j}$ can be approximated by the average of the corresponding fluxes evaluated at the nodes adjacent to the cell interface $(i + \frac{1}{2}, j)$:

$$\boldsymbol{F}_{i+\frac{1}{2},j} = \tfrac{1}{2}(\boldsymbol{F}_{i+1,j} + \boldsymbol{F}_{i,j}) \tag{26}$$

Moreover,

$$\boldsymbol{F} = \boldsymbol{f} n_x + \boldsymbol{g} n_y \tag{27}$$

where n_x and n_y are the direction cosines of the normal to the cell edge, and

$$\boldsymbol{f} = [\rho u, p + \rho u^2, \rho uv, \rho u h^0]^T \tag{28}$$

$$\boldsymbol{g} = [\rho v, \rho uv, p + \rho v^2, \rho v h^0]^T \tag{29}$$

In Eqs. (28) and (29) p, ρ, u, and v are, respectively, the pressure, density, and the two Cartesian components of the velocity vector, whereas e^0 and h^0 denote the total energy and total enthalpy per unit mass and can be expressed as

$$e^0 = [1/(\gamma - 1)](p/\rho) + \tfrac{1}{2}(u^2 + v^2)$$

$$h^0 = e^0 + p/\rho = [\gamma/(\gamma - 1)](p/\rho) + \tfrac{1}{2}(u^2 + v^2)$$

$$= a^2/(\gamma - 1) + \tfrac{1}{2}(u^2 + v^2)$$

where $a^2 = \gamma p/\rho$ is the sound speed.

Inverse Design of a Two-Dimensional Diffuser

The first two-dimensional test involves the same parameterization of the diffuser shape and the same definition of the objective function adopted for the one-dimensional case. The target area distribution for the two-dimensional case is defined by $\hat{A}(x) = -0.278x^3 + 0.417x^2 + 0.21$, which is the same as for the one-dimensional case but for a factor 5 introduced to reduce the angle of divergence of the two-dimensional diffuser. The target area distribution $\hat{A}$ has been used to determine the target pressure distribution $\hat{p}$ along the diffuser axis D over which the integral of the cost function I is evaluated.

The supersonic inlet Mach number is 1.3, and the subsonic exit pressure is 0.75. The exit-to-inlet area ratios for the one- and two-dimensional cases have the same value. Because the inlet and exit cross-section area are left unchanged by altering the design parameters, the shock has about the same strength no matter where along the diffuser it will settle. Moreover, the shock is essentially normal and is approximately aligned along the vertical grid lines.

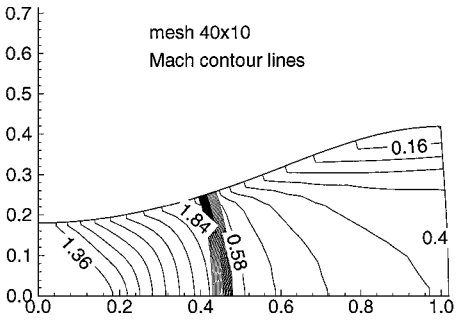

Fig. 6 Two-dimensional transonic diffuser: target iso-Mach lines.

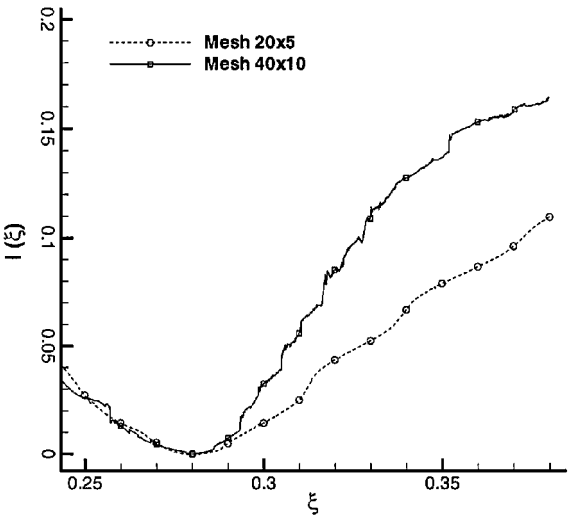

a) Objective function vs single design variable with 20 × 5 and 40 × 10 cell meshes

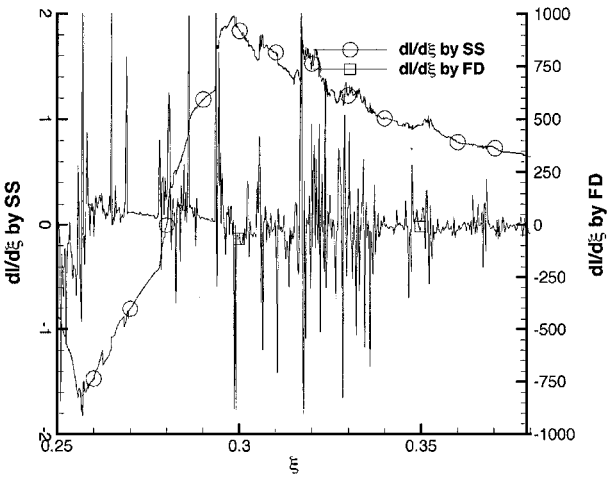

b) FD vs SSE sensitivity derivatives; 40 × 10 cell mesh

Fig. 7 Two-dimensional transonic diffuser.

Objective Function

We can demonstrate the nonsmooth and noisy nature of the objective function for this problem. We discretized the diffuser with a 20 × 5 and a 40 × 10 cell mesh. The target flow solution is reported in Fig. 6.

The case with a single design variable placed at the midpoint of the duct length (ξ_1 in Fig. 1) is utilized to obtain the objective function reported in Fig. 7a.

The figure reveals the wavy and noisy behavior of the objective function. On both sides of the target value ($\hat{\xi}_1 = 0.28$), there are jumps associated with the displacement of the shock from one cell to another and also large intervals where noise is present. The jumps have comparable height at both sides of the target because the shock,

as said before, has about the same strength independent of the diffuser shape. Comparing Fig. 7a with Fig. 3 illustrates that jumps caused by shocks are present in both the one-dimensional closed-form solution and the two-dimensional numerical solution, whereas noise is present only in the latter case because it has been ascertained that the noise is connected with poor convergence properties of the numerical solution. The problem is particularly noticeable when flux limiters are adopted.

FD vs SSE Sensitivity Derivatives

Next, we demonstrate the validity of the SSE method by comparing SSE and FD sensitivity derivatives. The results of the comparison are plotted in Fig. 7b, which shows the highly oscillatory behavior of the sensitivity derivatives $dI/d\xi_1$, computed as finite differences of the objective function of Fig. 7a and the smoother curve obtained by the SSE method. Because of this behavior, a FD-based optimization process is not likely to converge to the optimum design. In contrast, the SSE sensitivity derivatives may lead to a converged optimization because they are rather smooth everywhere and also they are positive at the right and negative at the left of the target value.

SSE Convergence Properties

To test the sensitivity derivatives obtained by the SSE method, we report four optimization results related to the transonic diffuser test case with the two-dimensional flow model, when one, five, and seven design variables are used to parameterize the diffuser shape.

One Design Variable

Two optimization runs based on Newton's method and starting from two different initial conditions are reported in Fig. 8. The figure shows the convergence history of the cross-section area at one-half of the duct $A_{1/2}$ (on the left-hand y axis) and of the base 10 logarithm of the objective function $\log(I)$ (on the right-hand y axis) vs the number of iterations. In both cases two to three iterations are sufficient to recover the target area and a drop in the objective function of seven orders of magnitude when a 40×10 cell mesh is used to solve the flow.

Five and Seven Design Variables

For the optimization of problems with several design variables, we adopted a sequential quadratic programming (SQP) algorithm. First, SQP was used to repeat the preceding optimizations with a single design variable. The computed results, not reported here for the sake of conciseness, showed a slowdown in convergence. We found that five to six iterations were necessary to obtain a drop in the objective function of four orders of magnitude.

Next, five and seven design variables have been considered: five design variables are located at $\frac{1}{8}$, $\frac{1}{4}$, $\frac{1}{2}$, $\frac{3}{4}$, and $\frac{7}{8}$ of the duct length, whereas the two further design variables of the seven-design-variable test case are located at $\frac{3}{8}$ and $\frac{5}{8}$ of the duct length. The optimization has been performed by employing a 40×10 cell mesh. The convergence history of $\log(I)$ is plotted in Fig. 9 for the five as well as for the seven-design-variable cases. In both cases five to six iterations are sufficient to recover the target area and a drop in the objective function of four orders of magnitude.

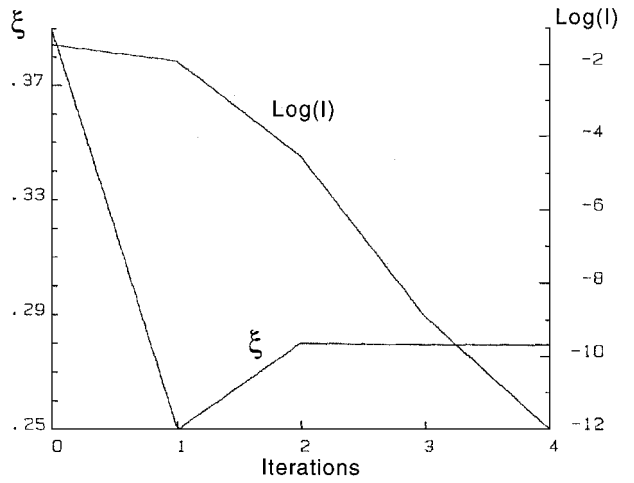

a) $\xi_0 = 0.378$

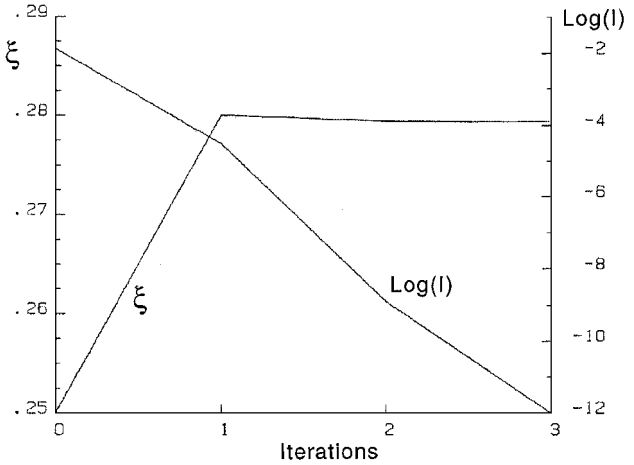

b) $\xi_0 = 0.250$

Fig. 8 Two-dimensional transonic diffuser: convergence history for one design variable and two different initial guesses.

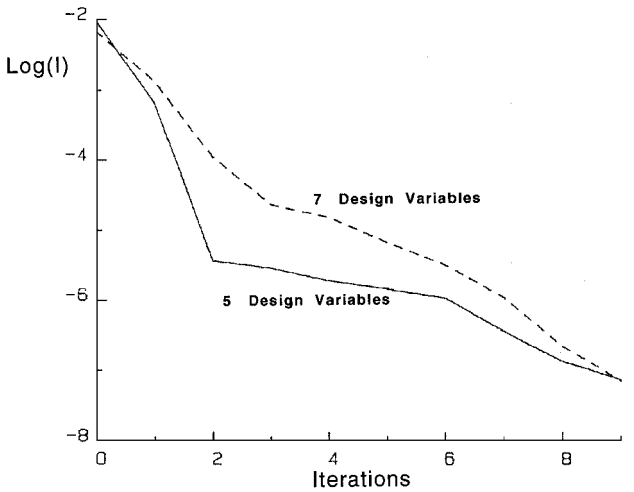

Fig. 9 Two-dimensional transonic diffuser: convergence history of $\log(I)$ for five (——) and seven (- - -) design variables.

Inverse Design of a Two-Dimensional Nozzle

The test case involves finding the (target) shape of the lower wall of the nozzle sketched in Fig. 10a under transonic and subsonic flow conditions.

The upper wall of the nozzle is at constant y, whereas the lower wall is expressed analytically as

$$y(x, \boldsymbol{\xi}) = \begin{cases} 0, & -0.5 \le x < 0 \\ \sum_{i=1}^{4} \xi_i x^{i-1}(x-1)^2, & 0 \le x < 1 \\ 0, & 1 \le x < 1.5 \end{cases} \tag{30}$$

The number of design variables is four ($N_v = 4$). The conditions at inflow are defined by enforcing unit values of total temperature and total pressure, whereas the subsonic and transonic flows are obtained by prescribing at the nozzle exit static pressure values of 0.9 and 0.5, respectively, as done in Ref. 14. The domain of integration involves a nonorthogonal, H-type, finite volume mesh. Calculations are performed by using grids of 20×10 and 40×20 cells.

The function F in the cost function of this test case is defined as the static pressure p and the domain D over which the cost function is evaluated is the lower wall of the nozzle.

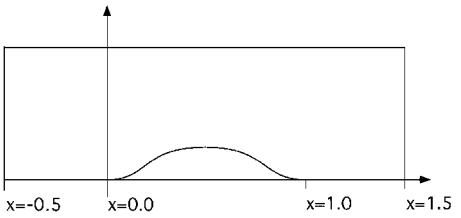

a) Nozzle geometry

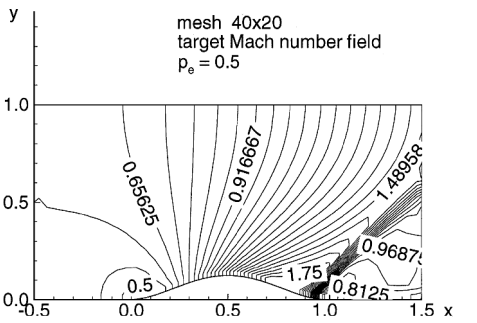

b) Target (transonic) iso-Mach lines; $\hat{\xi} = (2, 0, 0, 0)^T$

Fig. 10 Two-dimensional nozzle test case.

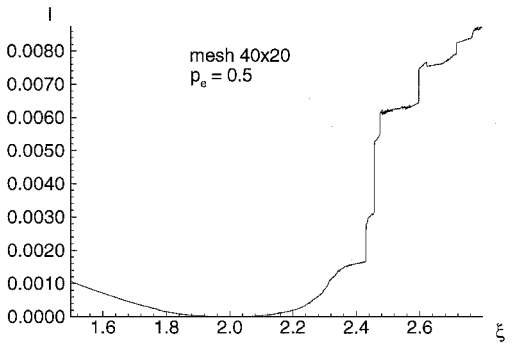

Fig. 11 Two-dimensional transonic nozzle: nonsmooth objective function.

Transonic Test Case

Transonic flow is obtained by enforcing a back pressure equal to 0.5 times the reservoir value. Figure 10b shows the target flow solution obtained by prescribing $\hat{\xi} = (2, 0, 0, 0)^T$. In this test case, the flow accelerates in the converging portion of the channel, becomes sonic at the throat, and finally becomes supersonic along the divergent portion of the nozzle. An oblique shock recompresses the flow to match the enforced pressure at the exit.

This case compared to the diffuser case requires a different formulation of the boundary conditions because it involves a subsonic inlet as opposed to the supersonic inlet of the diffuser. Moreover, the oblique shock leaving the computational domain at the nozzle exit makes the right boundary partly supersonic and partly subsonic. However, optimizing the nozzle seems to be a less demanding task than the transonic diffuser design because the oblique shock is weaker than a normal shock.

Objective Function

As the bump on the lower surface of the nozzle increases the obstruction of the nozzle, the nozzle throat area decreases, and the strength of the oblique shock increases. This is another difference from the diffuser case, where the shock strength is essentially constant and independent on the value of the design parameters. This is demonstrated by comparing the shape of the diffuser's (Fig. 7) and nozzle's (Fig. 11) objective functions. Jumps and noise are present at both side of the target value in the diffuser problem, whereas in the nozzle problem they develop only at the right side of the target value, which correspond to larger protrusions involving stronger oblique shocks.

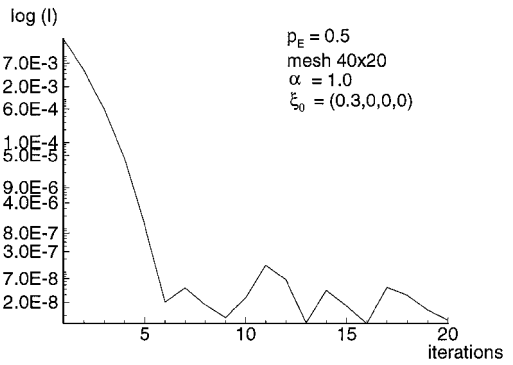

a) Objective function

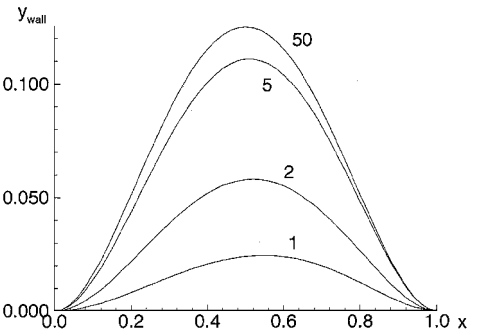

b) Bump geometry

Fig. 12 Two-dimensional transonic nozzle: convergence histories of objective function and bump geometry; mesh with 40 × 20 cells; initial guess $\xi_0 = (0.3, 0, 0, 0)^T$.

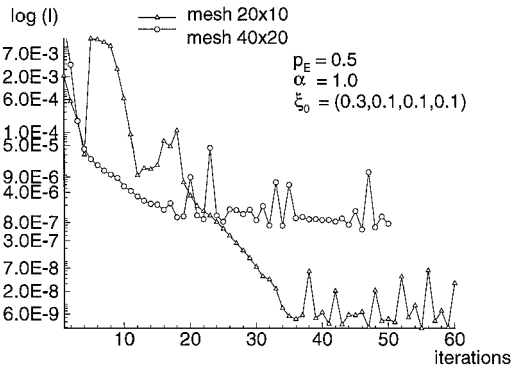

Fig. 13 Two-dimensional transonic nozzle: convergence history from the initial guess $\xi_0 = (0.3, 0.1, 0.1, 0.1)^T$. Meshes with 20 × 10 and 40 × 20 cells.

SSE Convergence Properties

An optimization search starting from the initial guess $\xi_0 = (0.3, 0, 0, 0)^T$, a viscosity coefficient $\alpha = 1$, and a 40×20 cell mesh drives the objective function below 10^{-9} in eight iterations (Fig. 12a). Figure 12b shows how the lower wall of the nozzle is modified during the optimization process.

Note that the initial guess corresponds with the target but for the first element ξ_1 of the design vector. Taking as initial guess $\xi_0 = (0.3, 0.1, 0.1, 0.1)^T$, whose elements are all different from the target, leads to a less regular convergence history (Fig. 13). Because the sensitivity of the design to changes of the coefficients of the polynomial (30) other than the first is weak, the optimization algorithm needs more iterations to adjust them to the target: 47 iterations are needed to reach an objective function of the order of 10^{-9} with a 20×10 cell mesh, whereas with a 40×20 cell mesh the objective function first decreases at a constant slope but eventually goes into an oscillation that prevents the objective function to drop below 10^{-7}.

In fact the SSE method resorts to the original objective function to drive the search for the optimum, and, therefore, it might happen

that close to the optimum the convergence might suffer because of the nonsmooth and noisy nature of the objective function, no matter that the sensitivity derivatives have been smoothed. However, the proposed method is mainly aimed at solving design problems with an engineering accuracy level. We checked numerically that this goal can be achieved by adopting standard optimization packages as well as the Newton-like algorithms because any general-purpose optimizer usually tries to choose the largest admissible change of the design parameters: this allows the skipping of the noise and the low-amplitude peaks of the nonsmooth objective function, until a narrow region wherein the optimum lies is reached. Moreover, in such a region the numerical optimum of the objective function is not uniquely defined and can slightly vary according to the noise level of the flow solution.

Subsonic Test Case

Numerical tests carried out in the subsonic flow regime, that is, with shock-free flows, demonstrated that the convergence properties of the smoothed sensitivity formulation are preserved—without any ad hoc treatment—even when the objective function is smooth. The computational cost associated is also equivalent because the procedure requires the same type and number of operations for both the smooth and nonsmooth cost function cases.

Conclusions

This paper analyzes the problem of optimizing the shape of a duct when the flow inside the duct develops shock waves that make the objective function nonsmooth or noisy.

The analysis carried out for the one-dimensional case, solved in closed-form, showed that the flow sensitivities involve a δ function when the shock is displaced following a perturbation of the design parameters.

To find one entropy-satisfying weak solution of the sensitivity equations under these circumstances, one can modify the sensitivity equations by adding a small artificial viscosity term.

The entropy-satisfying weak solution can be also obtained by first adding the artificial viscosity to the governing set of PDE and next by deriving the sensitivity equations from this modified set of governing PDE.

This modification is applied only to find the smoothed sensitivity derivatives, whereas the objective function is still computed by solving the flow by the most accurate solver available.

The smoothed sensitivity equations can be derived either by adopting the discrete direct or the adjoint formulations. The auxiliary flow solver is discretized by a cell-centered finite volume scheme.

The technique has been successfully validated in one- and two-dimensional test cases. The results showed that the convergence properties of the technique are preserved without loss of efficiency even when the flow is smooth.

Acknowledgments

The research has been supported by the Italian Agency MURST (Ministero dell'Università e della Ricerca Scientifica e Tecnologica). The authors acknowledge the contributions of M. Falcone (Scuola di Matematica "Castelnuovo," Università di Roma "La Sapienza") to the mathematical presentation of the technique. The author M. Valorani also acknowledges the collaboration of D. Girelli for carrying out the calculations of the two-dimensional test cases.

References

[1]Gill, P. E., Murray, W., and Wright, M. H., *Practical Optimization*, Academic, New York, 1981.

[2]Haug, E. J., Choi, K. K., and Komkov, V., *Design Sensitivity Analysis of Structural Systems, Mathematics in Science and Engineering*, Vol. 177, Academic, Orlando, FL, 1986.

[3]Pironneau, O., "On Optimum Design in Fluid Mechanics," *Journal of Fluid Mechanics*, Vol. 64, Pt. 1, 1974, pp. 97–110.

[4]Jameson, A., and Reuther, J., "Aerodynamic Design Via Control Theory," *Journal of Scientific Computing*, Vol. 3, 1988, pp. 233–260.

[5]Frank, P. D., and Shubin, G. R., "A Comparison of Optimization-Based Approaches for a Model Computational Aerodynamics Design Problem," *Journal of Computational Physics*, Vol. 98, No. 1, 1992, pp. 74–89.

[6]Iollo, A., Salas, M. D., and Ta'asan, S., "Shape Optimization Governed by the Euler Equations Using an Adjoint Method," Inst. for Computer Applications in Science and Engineering, Rept. 93-78, Hampton, VA, Nov. 1993.

[7]Narducci, R. P., Grossman, B., and Haftka, R. T., "Sensitivity Algorithms for an Inverse Design Problem Involving a Shock Wave," *Inverse Problems in Engineering*, Vol. 2, 1995, pp. 49–83.

[8]Narducci, R. P., Grossman, B., Valorani, M., Dadone, A., and Haftka, R. T., "Optimization Methods for Non-Smooth or Noisy Objective Functions in Fluid Design Problems," AIAA Paper 95-1648, June 1995.

[9]Valorani, M., and Dadone, A., "Sensitivity Derivatives for Non-Smooth or Noisy Objective Functions in Fluid Design Problems," *Numerical Methods for Fluid Dynamics*, Vol. 5, Clarendon, Oxford, 1995, pp. 605–613.

[10]Dadone, A., Valorani, M., and Grossman, B., "Optimization of 2D Fluid Design Problems with Non-Smooth or Noisy Objective Function," *Proceedings of the 3rd ECCOMAS Computational Fluid Dynamics Conference*, edited by J.-A. Desideri, C. Hirsch, P. Le Tallec, M. Pandolfi, and J. Periaux, Wiley, 1996, pp. 425–431.

[11]Borggard, J., and Burns, J., "A Sensitivity Equation Approach to Optimal Design of Nozzles," AIAA Paper 94-4274, Sept. 1994.

[12]Borggard, J., and Burns, J., "Algorithms for Flow Control and Optimization," *Optimal Design and Control*, edited by J. Borggaard, J. Burkardt, M. Gunzburger, and J. Peterson, Birkhäuser, Amsterdam, 1994, pp. 97–116.

[13]Borggard, J., Burns, J., Cliff, E., and Gunzburger, M., *Optimal Design and Control*, edited by J. Borggaard, J. Burkardt, M. Gunzburger, and J. Peterson, Birkhäuser, Amsterdam, 1994.

[14]Iollo, A., and Salas, M. D., "Contribution to Optimal Shape Design of Two-Dimensional Internal Flows with Embedded Shocks," *Journal of Computational Physics*, Vol. 125, No. 1, 1996, pp. 124–134.

[15]Roe, P. L., "Characteristic Based Schemes for the Euler Equations," *Annual Review of Fluid Mechanics*, Vol. 18, 1986, pp. 337–365.

K. Kailasanath
Associate Editor